Supplementary Information (SI) for New Journal of Chemistry.
This journal is © The Royal Society of Chemistry and the Centre National de la Recherche Scientifique 2026

Supplementary Information

Composition controlled metallic Sn-doped MoS_2 nanosheets for flexible and wearable temperature sensor

Tingting Liang,[a] Haolong Sun,[a] Tingting Zhu,[a] Daobo Tian,[a] Sen Liang,*[a] Xiaoshan Wang,*[a]
[a]Ningxia Key Laboratory of Photovoltaic Materials, School of Materials and New Energy, Ningxia University, Yinchuan 750021, P. R. China
Corresponding author: Sen Liang (liangsen@nxu.edu.cn); Xiaoshan Wang (xswang@nxu.edu.cn)

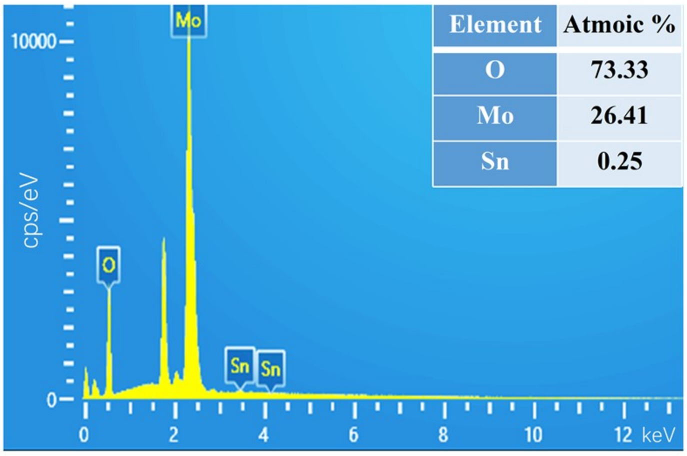

Element	Atmoic %
O	73.33
Mo	26.41
Sn	0.25

Fig. S1 The EDS spectrum of $Sn_{0.01}Mo_{0.99}O_3$ nanorods.

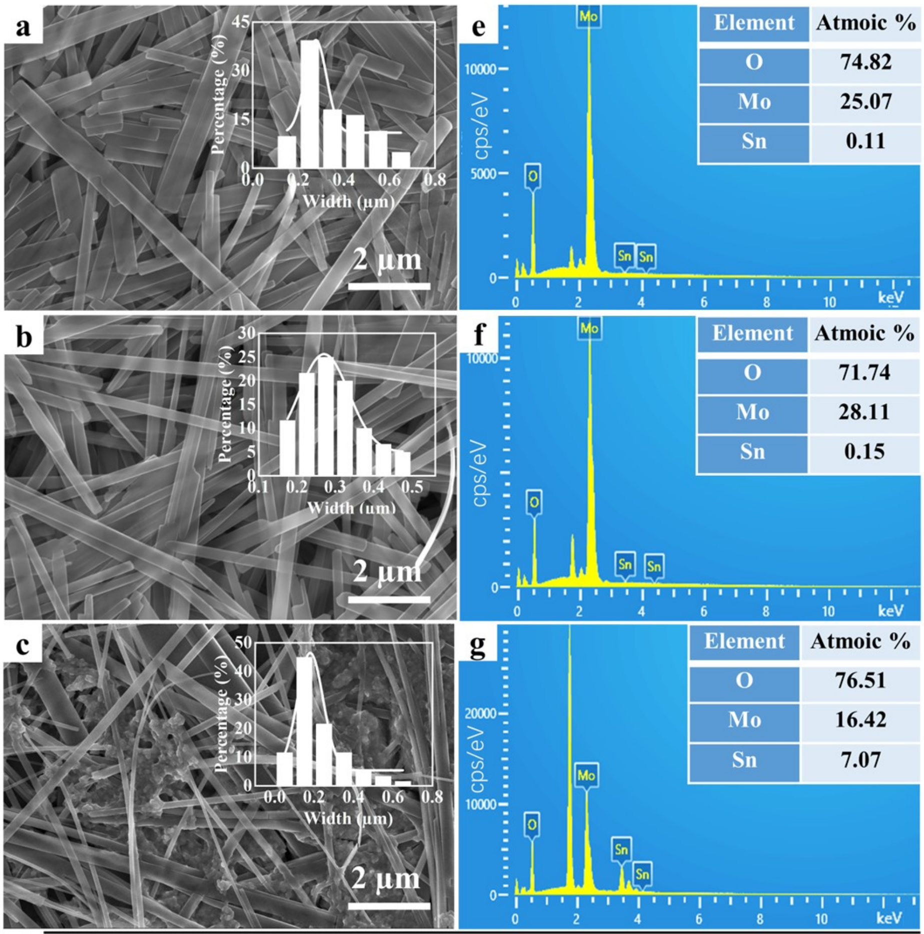

e

Element	Atmoic %
O	74.82
Mo	25.07
Sn	0.11

f

Element	Atmoic %
O	71.74
Mo	28.11
Sn	0.15

g

Element	Atmoic %
O	76.51
Mo	16.42
Sn	7.07

d

$SnCl_4•5H_2O$	0.3 mmol	0.6 mmol	0.9 mmol	1.2 mmol
Sn-doped MoO_3	$Sn_{0.004}Mo_{0.996}O_3$	$Sn_{0.005}Mo_{0.995}O_3$	$Sn_{0.01}Mo_{0.99}O_3$	$Sn_{0.3}Mo_{0.7}O_3$
Nanobelt width	0.34 μm	0.30 μm	0.28 μm	0.23 μm

Fig. S2 The SEM images and EDS spectra of (a,e) $Sn_{0.004}Mo_{0.996}O_3$, (b,f) $Sn_{0.005}Mo_{0.995}O_3$, (c,g) $Sn_{0.3}Mo_{0.7}O_3$ nanorods. (d) the average width of Sn-doped MoO_3 nanorods. Inset in a-d: the normal distribution diagram of $Sn_xMo_{1-x}O_3$ nanorods with different x values.

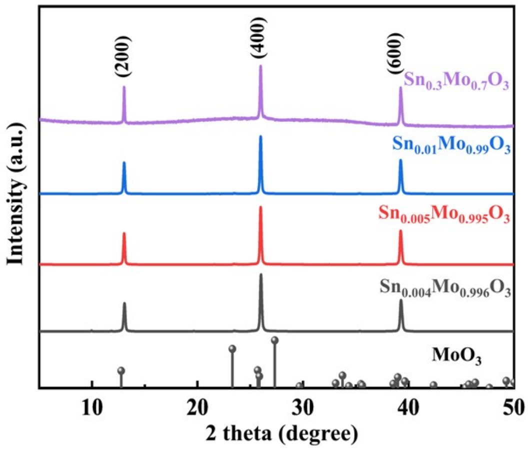

Fig. S3 The XRD patterns of $Sn_xMo_{1-x}O_3$ nanorods with different x value.

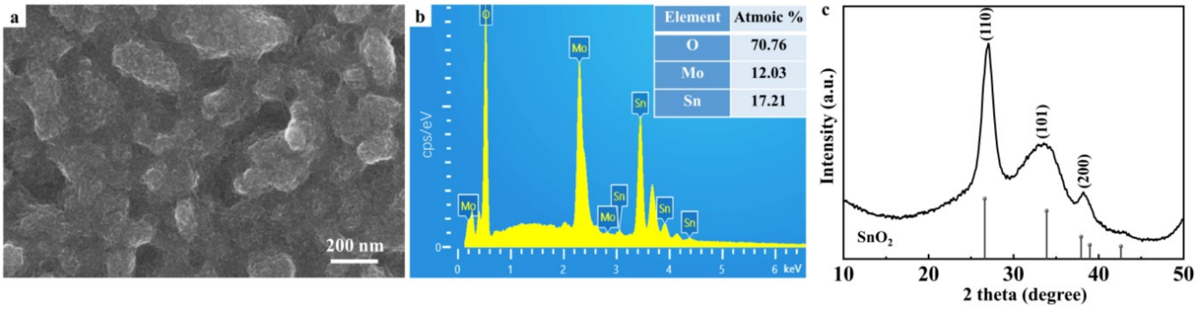

Element	Atmoic %
O	70.76
Mo	12.03
Sn	17.21

Fig. S4 (a) SEM image, (b) EDS spectrum, and (c) XRD pattern of Mo-doped SnO_2.

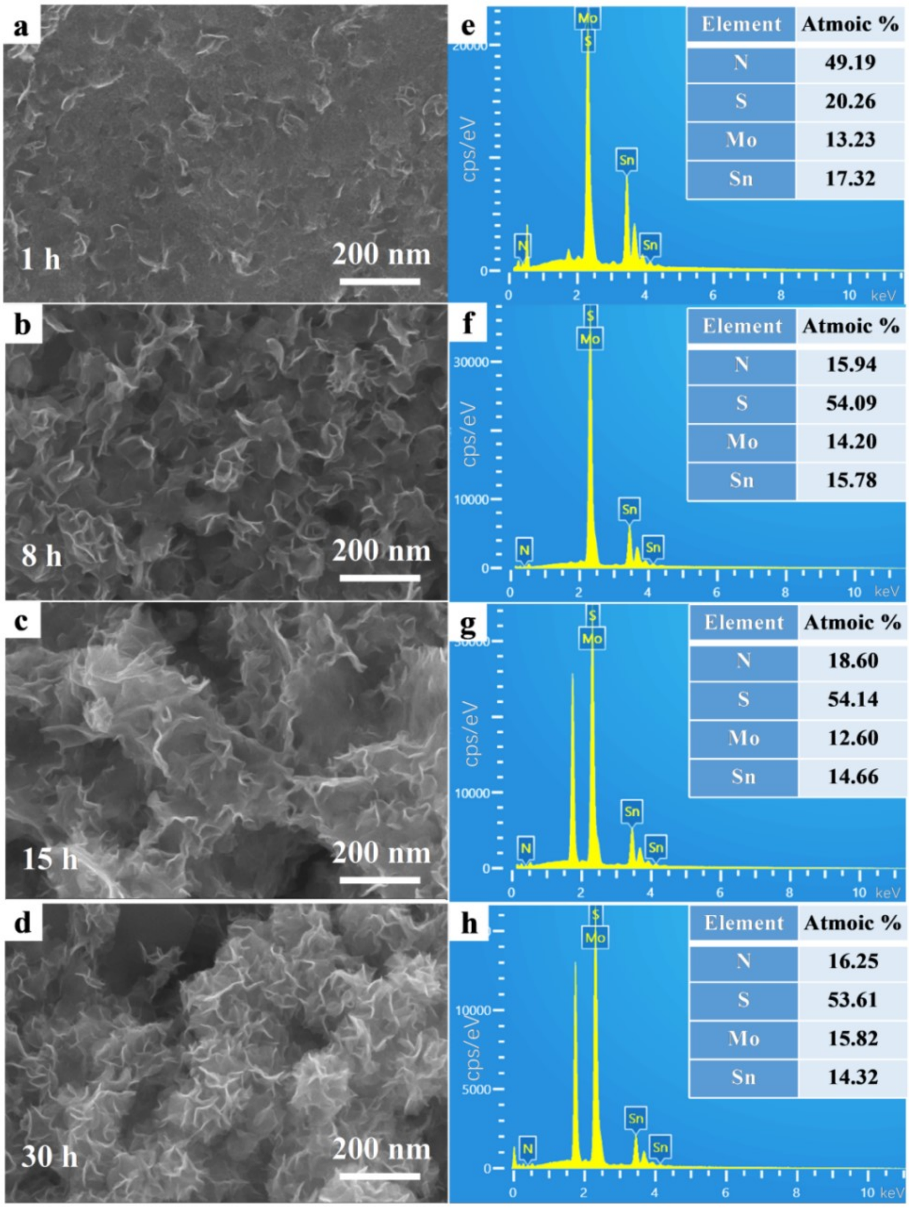

Element	Atmoic %
N	49.19
S	20.26
Mo	13.23
Sn	17.32

Element	Atmoic %
N	15.94
S	54.09
Mo	14.20
Sn	15.78

Element	Atmoic %
N	18.60
S	54.14
Mo	12.60
Sn	14.66

Element	Atmoic %
N	16.25
S	53.61
Mo	15.82
Sn	14.32

Fig. S5 The SEM images and EDS spectra of the intermediate products of the reaction. (a,e) reaction time: 1 h; (b,f) reaction time: 8 h; (c,g) reaction time: 15 h; (d,h) reaction time: 30 h.

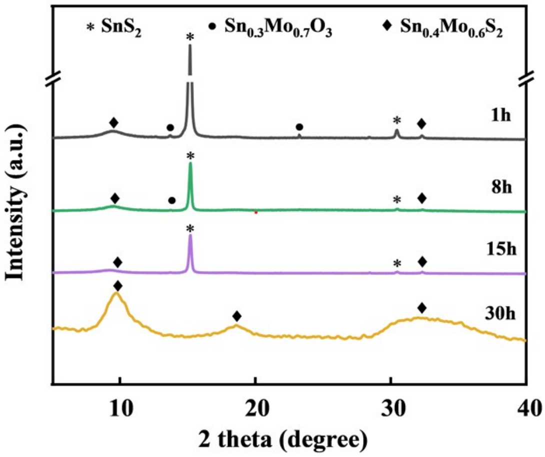

Fig. S6 The XRD patterns of the intermediate products of the reaction.

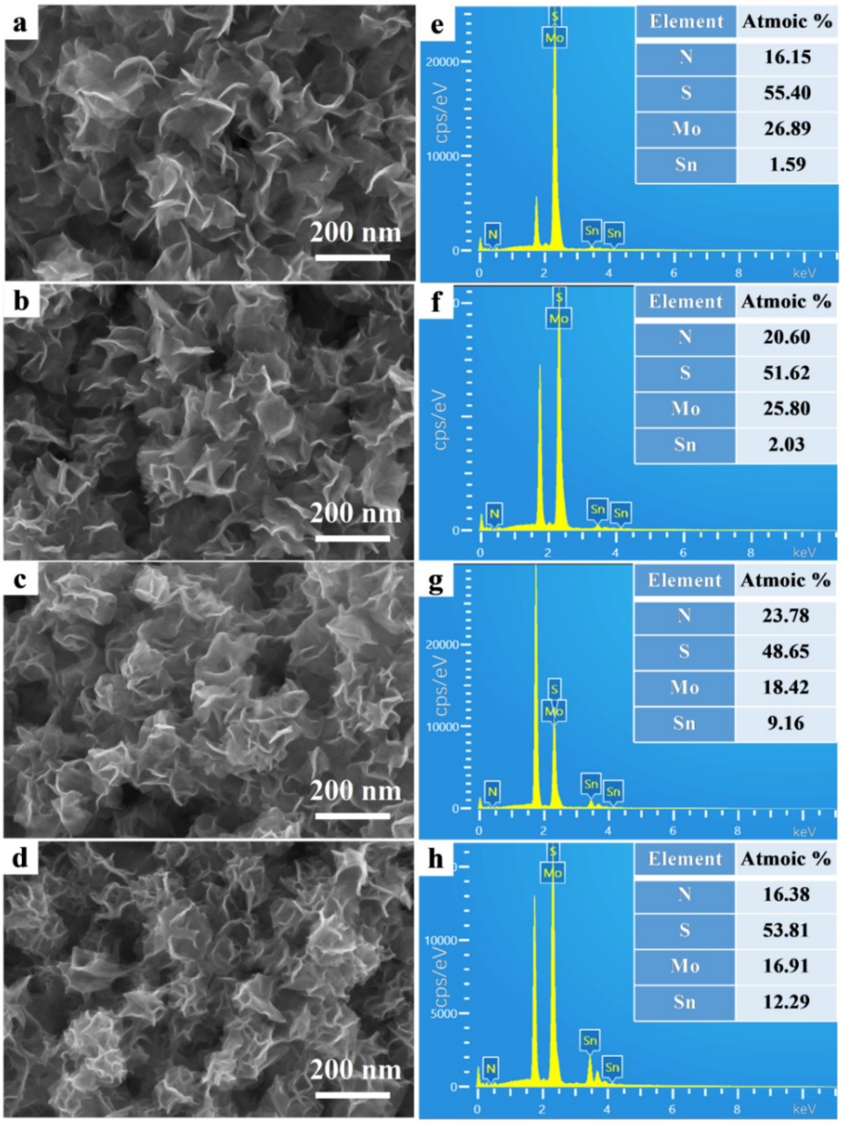

Element	Atmoic %
N	16.15
S	55.40
Mo	26.89
Sn	1.59

Element	Atmoic %
N	20.60
S	51.62
Mo	25.80
Sn	2.03

Element	Atmoic %
N	23.78
S	48.65
Mo	18.42
Sn	9.16

Element	Atmoic %
N	16.38
S	53.81
Mo	16.91
Sn	12.29

Fig. S7 The SEM images and EDS spectra of $Sn_xMo_{1-x}S_2$ nanosheets. (a,e) $Sn_{0.05}Mo_{0.95}S_2$, (b,f) $Sn_{0.07}Mo_{0.93}S_2$, (c,g) $Sn_{0.3}Mo_{0.7}S_2$, (d,h) $Sn_{0.4}Mo_{0.6}S_2$.

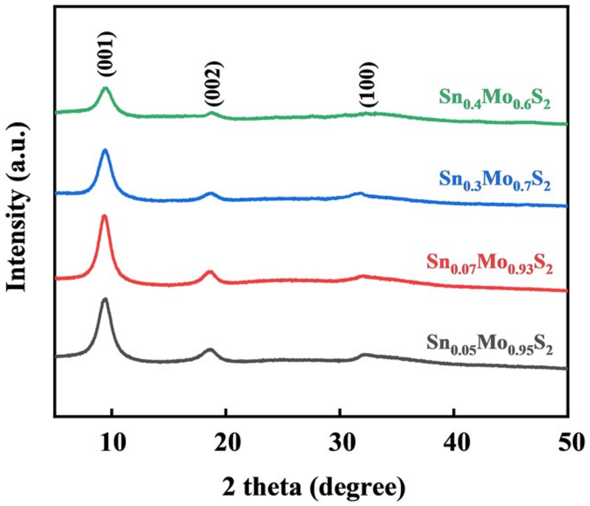

Fig. S8 The XRD patterns of $Sn_xMo_{1-x}S_2$ nanosheets with different x values.

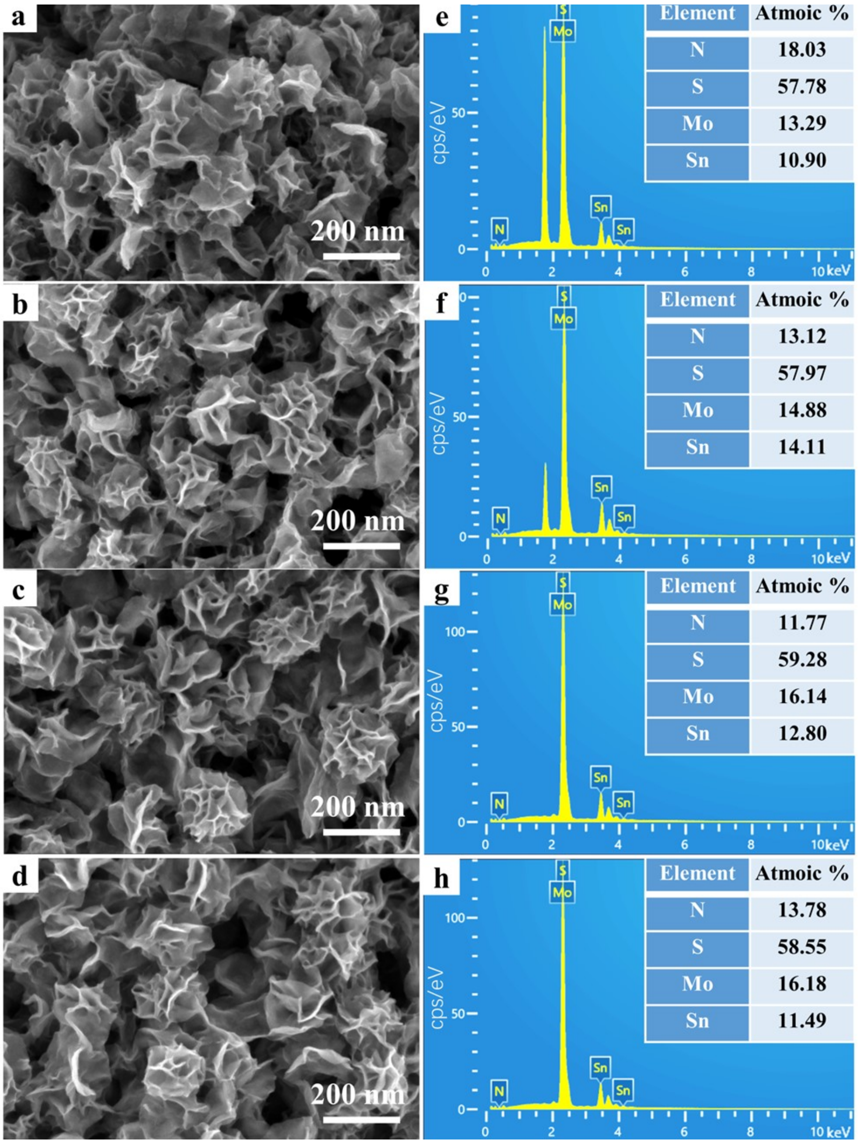

(e)

Element	Atmoic %
N	18.03
S	57.78
Mo	13.29
Sn	10.90

(f)

Element	Atmoic %
N	13.12
S	57.97
Mo	14.88
Sn	14.11

(g)

Element	Atmoic %
N	11.77
S	59.28
Mo	16.14
Sn	12.80

(h)

Element	Atmoic %
N	13.78
S	58.55
Mo	16.18
Sn	11.49

Fig. S9 The SEM images and EDS spectra of $Sn_xMo_{1-x}S_2$ nanosheets synthesized by $Sn_{0.3}Mo_{0.7}O_3$ nanorods with different proportions. (a, e) 9 mg of $Sn_{0.3}Mo_{0.7}O_3$, (b, f) 27 mg of $Sn_{0.3}Mo_{0.7}O_3$, (c, g) 45 mg of $Sn_{0.3}Mo_{0.7}O_3$, (d, h) 63 mg of $Sn_{0.3}Mo_{0.7}O_3$.

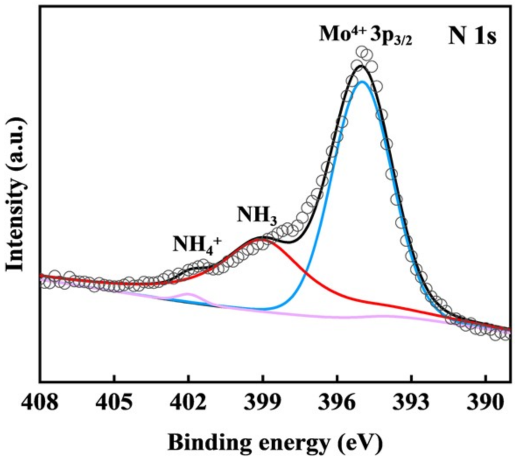

Fig. S10 The XPS N 1s spectrum of $Sn_{0.4}Mo_{0.6}S_2$ nanosheets.

Table S1 Sensing performance of various temperature sensors.

Material type	Material	Sensor type	Fabrication method	Temperature range	Sensitivity	Stretchability	Ref.
Carbon material	rGO/PET	NTC	Inkjet printing	25-85 °C	-0.0148 °C^{-1}	Flexible	1
	rGO/PET	NTC	Air spray coating	30-100 °C	-0.6345% °C^{-1}	Flexible	2
	rGO fiber	NTC	Wet spinning	30-80 °C	-0.636% °C^{-1}	Flexible	3
	PEI-rGO/polyimide (PI)	NTC	Spray coating	25-45 °C	-0.013 °C^{-1}	Bending angle:40°	4
	GO	PTC	Laser scan	30-100 °C	0.0037 °C^{-1}	Flexible	5
	All-elastomeric TS-gated device	PTC	-	30-80 °C	0.0134 °C^{-1}	Flexible	6
	SWCNT TFT	NTC	-	16-55 °C	-0.01435 °C^{-1}	Flexible	7
	SWCNTs	NTC	-	30-40 °C	-0.007 °C^{-1}	Flexible	8
	ACNF	PTC	Electrospinning	-	0.0152 ℃$^{-1}$	Flexible	9
	Ag-MWCNTs/PEDOT：PSS	NTC	Laser radiation	25-80 °C	-0.0045 ℃$^{-1}$	Flexible	10
MXenes	PEDOT：PSS/$Ti_3C_2T_x$	NTC	-	-	-	Flexible	11
	CNTs/MXene	NTC	-	-20-220 °C	-0.0052 ℃$^{-1}$	Flexible	12
	MXene/SA@CS	PTC	Aerosol jet printing	-	0.0108 ℃$^{-1}$	Flexible	13
	MXene/TOCNF/PVA	NTC	-	-	-0.0132 ℃$^{-1}$	Flexible	14
Metal material	V_2O_5 NWs	NTC	-	-	-0.015% ℃$^{-1}$	Flexible	15
	Al_2O_3@Cu NWs/PVDF	PTC	-	0-120 °C	0.0033 °C^{-1}	Flexible	16
	AgNPs/CA/PVA	NTC	-	35-40 °C	-0.08 °C^{-1}	Flexible	17
	AgNWs-PI	PTC	Filtration	-20-20 °C	0.0028-0.0033°C^{-1}	Flexible	18
	S-CNPs	NTC	-	15-85 °C	-0.0073 °C^{-1}	Flexible	19
	NiO NPs	PTC	-	25 -70 °C	0.004 °C^{-1}	Flexible	20
	Ni fibers	PTC	-	0-100 °C	0.0048 °C^{-1}	Flexible	21
Semiconductor	In_2O_3	NTC	Screen printing	25-700 °C	-226.7 μV °C^{-1}	Flexible	22
	MoS_2	NTC	Inkjet printing	30-70 °C	-0.0095-（-0.0102） °C^{-1}	Flexible	23
	Large-area MoS_2	NTC	-	38-42 °C	-0.0098 °C^{-1}	-	24
	Flexible monolayer MoS_2	PTC	CVD	27-120 °C	0.01-0.02 K^{-1}	Flexible	25
	MWCNT@MoS_2	NTC	-	298-373 K	-0.0062 K^{-1}	-	26
	Si_3N_4-coated MoS_2	PTC	LPCVD	25-550 ℃	0.0089 ℃$^{-1}$	-	27
	$Sn_{0.4}Mo_{0.6}S_2$ nanosheets	NTC		15-55 °C	-0.020 °C^{-1}	Flexible	This work

Notes: Negative temperature coefficient (NTC); Positive temperature coefficient (PTC).

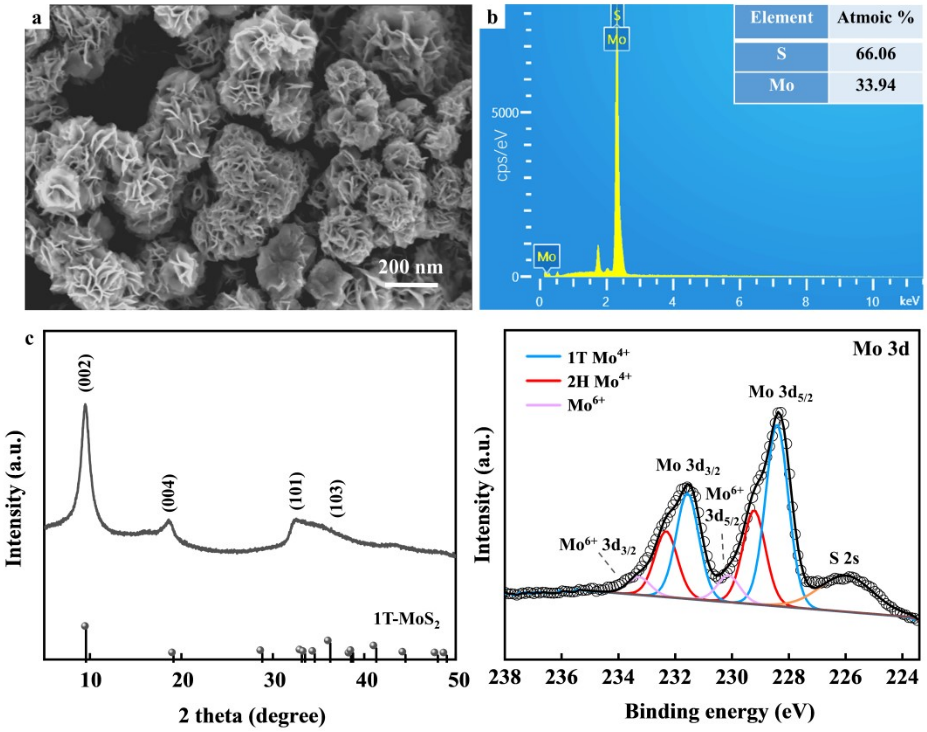

Fig. S11 (a) SEM image, (b) EDS spectrum, (c) XRD pattern, and (d) XPS Mo 3d spectra of 1T-MoS_2 nanosheets.

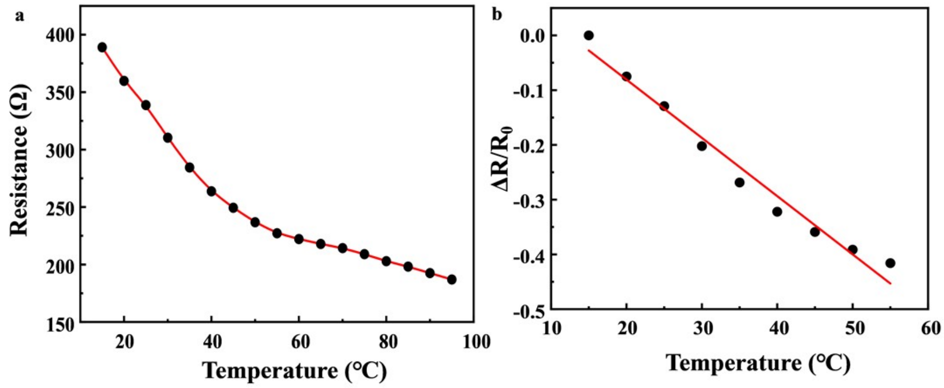

Fig. S12 (a) The resistance curve of the 1T-MoS_2 sensor varies with temperature. (b) Electrical response of the 1T-MoS_2 sensor in the temperature range of 15-55 °C.

Table S2 Resistance range of various temperature sensors.

Sensing materials	Resistance range (kΩ)	Ref.
$Sn_{0.4}Mo_{0.6}S_2$ anosheets	6-26	This work
Pt	0.109-0.11	[28]
Ni	0.109-0.131	[29]
SiC	0.7-10.6	[30]
$BaTiO_3$	0.01-1	[31]

Graphene	0.0036-23.8	[32]

References

1. D. Kong, L. T. Le, Y. Li, J. L. Zunino and W. Lee, *Langmuir*, 2012, **28**, 13467-13472.
2. G. Liu, Q. Tan, H. Kou, L. Zhang, J. Wang, W. Lv, H. Dong and J. Xiong, *Sensors*, 2018, **18**,1424-8220.
3. F. Li, H. Xue, X. Lin, H. Zhao and T. Zhang, *ACS Appl. Mater. Interfaces*, 2022, **14**, 43844-43852.
4. Q. Liu, H. Tai, Z. Yuan, Y. Zhou, Y. Su and Y. Jiang, *Adv. Mater. Technol.*, 2019, **4**, 1800594.
5. R. Chen, T. Luo, D. Geng, Z. Shen and W. Zhou, *Carbon*, 2022, **187**, 35-46.
6. T. Q. Trung, L. T. Duy, S. Ramasundaram and N.-E. Lee, *Nano Res.*, 2017, **10**, 2021-2033.
7. C. Zhu, A. Chortos, Y. Wang, R. Pfattner, T. Lei, A. C. Hinckley, I. Pochorovski, X. Yan, J. W. F. To, J. Y. Oh, J. B. H. Tok, Z. Bao and B. Murmann, *Nat. Electron.*, 2018, **1**, 183-190.
8. G. Zhu, F. Wang, L. Chen, C. Wang, Y. Xu, J. Chen, X. Chang and Y. Zhu, *Compos. Sci. Technol.*, 2022, **217**, 109133.
9. J.-H. Lee, H. Chen, E. Kim, H. Zhang, K. Wu, H. Zhang, X. Shen, Q. Zheng, J. Yang, S. Jeon and J.-K. Kim, *Mater. Horiz.*, 2021, **8**, 1488-1498.
10. Z. Zhang, Q. Li, L. Xu, W. Tian and Z. Li, *ACS Appl. Mater. Interfaces*, 2024, **16**, 6078-6087.
11. R. Hu, J. Li, F. Wu, Z. Lu and C. Deng, *Chem. Eng. J.*, 2024, **491**, 152135.
12. B. Sun, G. Xu, X. Ji, Z. Yang, C. Guan, S. Chen, X. Chen, Y. Ma, Y. Yu and J. Feng, *Sensor. Actuat. A:-Phys.*, 2024, **368**, 115059.
13. B. Huang, S. Wu, J. Liu, J. Liu, B. Peng and Z. Zhou, *Chem. Eng. J.*, 2025, **519**, 165403.
14. S. Hao, Q. Fu, L. Meng, F. Xu and J. Yang, *Nat. Commun.*, 2022, **13**, 6472.
15. H. Nakamura, R. Ezaki, G. Matsumura, C.-C. Chung, Y.-C. Hsu, Y.-R. Peng, A. Fukui, Y.-L. Chueh, D. Kiriya and K. Takei, *ACS Appl. Mater. Interfaces*, 2024, **16**, 19198-19204.
16. L. Zhao, P. Yang, S. Shi, X. Wang and S. Yu, *Chem. Eng. J.*, 2023, **473**, 145156.
17. L. Chen, Y. Xu, Y. Liu, J. Wang, J. Chen, X. Chang and Y. Zhu, *ACS Appl. Mater. Interfaces*, 2023, **15**, 24923-24932.
18. D.-Y. Youn, U. Jung, M. Naqi, S.-J. Choi, M.-G. Lee, S. Lee, H.-J. Park, I.-D. Kim and S. Kim, *ACS Appl. Mater. Interfaces*, 2018, **10**, 44678-44685.
19. H. K. Sadhanala, S. Senapati and K. K. Nanda, *Carbon*, 2018, **133**, 200-208.
20. J. Shin, B. Jeong, J. Kim, V. B. Nam, Y. Yoon, J. Jung, S. Hong, H. Lee, H. Eom, J. Yeo, J. Choi, D. Lee and S. H. Ko, *Adv. Mater.*, 2020, **32**, 1905527.
21. M. D. Husain and R. Kennon, *Fibers*, 2013, **1**, 2-10.
22. Z. Liu, B. Tian, B. Zhang, Z. Zhang, J. Liu, L. Zhao, P. Shi, Q. Lin and Z. Jiang, *Micromachines*, 2021, **12**.
23. Y. Lu, J. Wang, J. He, L. Zou, D. Zhao and S. Song, *ACS Appl.Mater. Interfaces*, 2022, **14**, 29250-29260.
24. W. Li, M. Xu, J. Gao, X. Zhang, H. Huang, R. Zhao, X. Zhu, Y. Yang, L. Luo, M. Chen, H. Ji, L. Zheng, X. Wang and W. Huang, *Adv. Mater.*, 2023, **35**, 2207447.
25. A. Daus, M. Jaikissoon, A. I. Khan, A. Kumar, R. W. Grady, K. C. Saraswat and E. Pop, *Nano Lett.*, 2022, **22**, 6135-6140.
26. F. Khan, C. M. Julien and S. S. Islam, *FlatChem*, 2023, **40**, 100521.
27. L. Kong, Y. Li, Y. Wang and T. Deng, *Nanotechnology*, 2025, **36**, 015501.
28. M. Li, Y. Wang, Y. Guo, Y. Qiao, S. Zhang, J. Liu, Z. Zhang, D. Cui, Y. Chen, D. Liu and C. Xue, *IEEE Sens. J.*, 2025, **25**, 10628-10636.
29. X. Huang, W. Xiang, C. Li, M. Guo, G. Zhang, Y. Huang, Y. Liu, W. Yang and C. Wang, *Adv. Mater. Technol.*, 2023, **8**, 2201093.
30. W. Wu, X. Wang, L. Liu, Y. Wang, Y. Li and H. Pu, *MRS Commun.*, 2025, **15**, 1479-1484.
31. J. G. Bell, T. Graule and M. Stuer, *Appl. Phys. Rev.*, 2021, **8**, 031318.
32. V. Šedajová, J. Štulík, P. Jakubec and M. Otyepka, *Adv.Electron. Mater.*, 2024, **10**, 2400052.